

A note on groups of a family of hyperbolic tessellations

Anthony Gasperin¹, Maurice Margenstern²

¹ Laboratoire d'Informatique Théorique, TCS,
Université de Genève.

e-mail : anthony.gasperin@unige.ch, anthony.gasperin@gmail.com

² Laboratoire d'Informatique Théorique et Appliquée, EA 3097,
Université de Lorraine, LITA EA3097,

Campus du Saulcy,
57045 Metz Cedex, France,

e-mail : maurice.margenstern@univ-lorraine.fr, margenstern@gmail.com

Abstract

In this paper we study the word problem of groups corresponding to tessellations of the hyperbolic plane. In particular using the Fibonacci technology developed by the second author we show that groups corresponding to the pentagrid or the heptagrid are not automatic.

1 Introduction

The word problem for a finitely generated group is the algorithmic problem of deciding whether two words in the generators represent the same element. Dehn in [23] suggested that it was an important area of study in its own right. In [24] he gave an algorithm that solves it for the fundamental group of closed orientable two-dimensional manifolds of genus greater or equal than two. Then the Dehn's algorithm has been extended and applied to a wide range of group theoretic problems. In 1955 Novikov [19] showed that there exists a finitely presented group with an undecidable word problem. A different proof is given by Boone in 1958. In cases where the problem is decidable it is interesting to study to which class the problem belongs. In particular it is known that hyperbolic groups have word problem recognizable by a finite state automata. Groups with context-free word problem are precisely virtually free groups ([21],[22]) and their word problem is in fact deterministic context-free. Sapir, Birget and Rips obtained a characterization of groups with **NP** word problem: a finitely generated group has word problem in **NP** if and only if it embeds into a finitely presented groups with polynomial Dehn function. In this paper we study the word problem of groups that corresponds to the pentagrid or the heptagrid. That is we consider the groups which have a Cayley graph that represents the pentagrid or the

heptagrid. The study considers of the Fibonacci technology developed by the second author [16],[17]. The technique allows one to find the location of a cell and its neighbours in the pentagrid. The Fibonacci technology has also some interesting algorithmic properties. For example, in [15] an algorithmic description of contour words is emphasized and concluded using the Fibonacci technology. We shall show that considering these algorithmic properties leads to a characterization of the groups we study.

2 An abstract on hyperbolic geometry

In order to simplify the approach for the reader, we shall present a model of the hyperbolic plane and simply refer to the literature for a more abstract, purely axiomatic exposition.

As it is well known, hyperbolic geometry appeared in the first half of the XIXth century, in the last attempts to prove the famous parallel axiom of Euclid's *Elements* from the remaining ones. Hyperbolic geometry was yielded as a consequence of the repeated failure of such attempts. Lobachevsky and, independently, Bolyai, discovered a new geometry by assuming that in the plane, from a point out of a given line, there are at least two lines which are parallel to the given line. Later, during the XIXth century, models were discovered that gave implementations of the new axioms. The constructions of the models, all belonging to Euclidean geometry, proved by themselves that the new axioms bring no contradiction to the other ones. Hyperbolic geometry is not less sound than Euclidean geometry is. It is also no more sound, in so far as much later, models of the Euclidean plane were discovered in the hyperbolic plane.

Among the models of hyperbolic geometry, Poincaré's models met with great success because in these models, hyperbolic angles between lines coincide with the Euclidean angles of their supports. In this paper, we take Poincaré's disc as a model of the hyperbolic plane.

2.1 Lines of the hyperbolic plane and angles

In Poincaré's disc model, the hyperbolic plane is the set of points lying inside a fixed open disc of the Euclidean plane. The points which are on the border of the disc do not belong to the hyperbolic plane. However they play an important role in the model and they are called **points at infinity**. We shall also call their set the **border circle**.

The lines of the hyperbolic plane in Poincaré's disc model are the trace in the disc of or circles, orthogonal to the border circle. We say that such a circle *supports* the hyperbolic line, *h*-line for short, and sometimes simply *line* when there is no ambiguity.

Poincaré's unit disc model of the hyperbolic plane makes an intensive use of some properties of the Euclidean geometry of circles, see [8] for an elementary presentation of the properties which are needed for our paper.

It is easy to see that an h -line defines two points at infinity by the intersection of its Euclidean support with the unit circle. They are called points at infinity of the h -line. The following easily proved properties will often be used: any h -line has exactly two points at infinity; two points at infinity define a unique h -line passing through them; a point at infinity and a point in the hyperbolic plane uniquely define a h -line.

The angles between h -lines are defined as the Euclidean angle between the tangents to the arcs which are taken as the support of the corresponding h -lines. This is one reason for choosing that model: hyperbolic angles between h -lines are, in a natural way, the Euclidean angle between the corresponding supports. In particular, orthogonal circles support perpendicular h -lines.

In the hyperbolic plane, given a line, say ℓ , and a point A not lying on ℓ , there are infinitely many lines passing through A which do not intersect ℓ . In the Euclidean plane, two lines are parallel if and only if they do not intersect. If the points at infinity are added to the Euclidean plane, parallel lines are characterized as the lines passing through the same point at infinity. Hence, as for lines, to have a common point at infinity and not to intersect is the same property in the Euclidean plane.

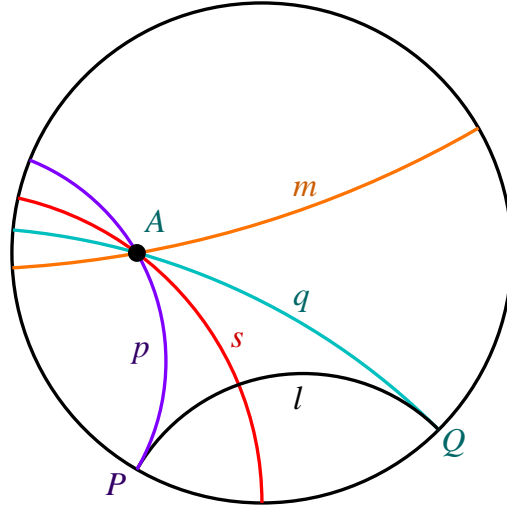


FIGURE 1 The h -lines p and q are parallel to the h -line ℓ , with points at infinity P and Q . The h -line s cuts ℓ and the h -line m is non-secant with ℓ .

This is not the case in the hyperbolic plane, where two lines may not intersect and have no common point at infinity. We shall distinguish these two cases by calling **parallel**, h -lines that share a common point at infinity, and **non secant**, h -lines which have no common point at all neither in the hyperbolic plane nor at

infinity. So, considering the situation illustrated by Figure 1, there are exactly two h -lines parallel to a given h -line ℓ which pass through a point A not lying on ℓ and infinitely many ones which pass through A but are non-secant with ℓ . This is easily checked in Poincaré's disc model, see Figure 1. Some authors call *hyperparallel* or *ultraparallel* lines which we call *non-secant*.

Another aspect of the parallel axiom deals with the sum of interior angles at the vertices of a polygon. In the Euclidean plane, the sum of angles of any triangle is exactly π . In the hyperbolic plane, this is no more true: the sum of the angles of a triangle is *always less* than π . The difference from π is, by definition, the **area** of the triangle in the hyperbolic plane. Indeed, one can see that the difference of the sum of the angles of a triangle from π has the additive property of a measure on the set of all triangles. As a consequence, there is no rectangle in the hyperbolic plane. Consequently two non-secant lines, say ℓ and m , have, at most, one common perpendicular. It can be proved that this is the case: two non-secant lines of the hyperbolic plane have exactly one common perpendicular.

It can be added that parallel h -lines have no common perpendicular. Consider the following problem of Euclidean geometry:

- (P) Let α, β, γ be positive real numbers such that $\alpha + \beta + \gamma = \pi$ and let be given two lines ℓ, m intersecting in A with angle α . How many triangles ABC can be constructed with $B \in \ell, C \in m$ and BC making angle β in B with ℓ ?

The answer is clearly: infinitely many. That property of the Euclidean plane defines the notion of *similarity*.

Another consequence of the non-validity of Euclid's axiom on parallels in the hyperbolic plane is that there is no notion of similarity in that plane: *if α, β, γ are positive real numbers such that $\alpha + \beta + \gamma < \pi$, ℓ and m are h -lines intersecting in A with angle α , there are exactly two triangles ABC such that $B \in \ell, C \in m$ and BC makes angle β in B with ℓ and angle γ in C with m . Each of those triangles is determined by the side of ℓ with respect to A in which B is placed.*

2.2 Reflections in a h -line

Any h -line, say ℓ , defines a **reflection** in that line denoted by ρ_ℓ . Let Ω be the center of the Euclidean support of ℓ , R its radius. Two points M and M' are **symmetric** with respect to ℓ if and only if Ω, M and M' belong to the same Euclidean line and if $\Omega M \cdot \Omega M' = R^2$. Moreover, M and M' do not lie in the same connected component of the complement of ℓ in the unit disc. We also say that M' is obtained from M by the reflection in ℓ . It is clear that M is obtained from M' by the same reflection.

All the transformations of the hyperbolic plane that we shall later consider are reflections or constructed as products of reflections.

By definition, an **isometry** of the hyperbolic plane is a finite product of reflections. Two segments AB and CD are called *equal* if and only if there is

an isometry transforming AB into CD .

It is proved that finite products of reflections can be characterized as either a single reflection or the product of two reflections or the product of three reflections. In our sequel, we will mainly be interested by single reflections or products of two reflections. We shall briefly mention products of three reflections in section 6. The set which contains the identity and the product of two reflections constitutes a group which is called the **group of motions**.

At this point, we can compare *reflections* in a line in the hyperbolic plane with symmetries with respect to a line in the Euclidean plane. Indeed, these respective transformations share many properties on the objects on which they respectively operate. However, there is a very deep difference between the isometries of the Euclidean plane and those of the hyperbolic plane: while in the first case, the group of motions possesses non trivial normal subgroups, in the second case, this is no more the case: the group is simple.

The product of two reflections with respect to lines ℓ and m is a way to focus on that difference. In the Euclidean case, according to whether ℓ and m do intersect or are parallel, the product of the two corresponding symmetries is a rotation around the point of intersection of ℓ and m , or a shift in the direction perpendicular to both ℓ and m . In the hyperbolic case, if h -lines ℓ and m intersect at a point A , the product of the corresponding reflections is again called a rotation around A as far as the obtained transformation can be considered as what is intuitively called a rotation. But, if ℓ and m do not intersect, there are two cases: either ℓ and m intersect at infinity, or they do not intersect at all. This gives rise to different cases of shifts. The first one, called **ideal rotation**, is a kind of degenerated rotation, as in the Euclidean case, and the second one is called **hyperbolic shift** or simply **shift** along the common perpendicular to ℓ and m . Such a shift can be characterized by the image P' of any point P on the common perpendicular, say n . We shall speak of the shift along n transforming P into P' . When n , P and P' are clear from the context, they are omitted and we simply speak about the shift.

It can be proved that for any couple of two h -lines ℓ and m , there is an h -line n such that ℓ and m are exchanged in the reflection in n . In the case when ℓ and m are non-secant, n is the perpendicular bisector of the segment that joins the intersections of ℓ and m with their common perpendicular.

3 The group-theoretic approach

It is well known that the notion of reflection in the Euclidean geometry is an important case which illustrates the power of the theory of groups which operate on a space.

An important notion which applies this general idea to many geometrical settings is the notion of Cayley graph.

Consider a directed graph (V, A) , where V is the set of vertices and A is the set of arcs and assume that the degree of the graph is constant and finite. We say that (V, A) is the **Cayley graph** of some group G if and only if G is

finitely generated, and there is a labelling of the arcs by generators of G or their inverses such that:

- for any arc α from v to w , γ labels α if and only if $\gamma(v) = w$;
- for any vertex v , the labels which are set on the arcs starting from v or arriving to v generate G ; they constitutes the **labels around** v ;
- the set of labels around v is the same for all the vertices of V .

A **Cayley graph** is a directed graph (V, A) for which there is a finitely generated group G such that (V, A) is the Cayley graph of (V, A) .

The three regular tilings of the Euclidean plane are examples of Cayley graphs of groups. More important, they are Cayley graphs of groups which are closely related with the motions which leave the tiling invariant.

A classical example is the example of the hexagonal tiling of the Euclidean plane. Fix A a vertex and call a, b, c the three shifts which transform A into the other end of the arc starting from A or arriving to A . It is not difficult to see that we can identify any vertex by a word on the alphabet $\{a, b, c, a^{-1}, b^{-1}, c^{-1}\}$, and we have a simplification rule given by $ab^{-1}ca^{-1}b = 1$, where 1 denotes the identity transformation.

It is plain that going from any vertex v to another one w defines a word whose letters label the **path** from v to w . It is no less plain that there are infinitely many words that can be associated in that way for a given couple of points and even a big number of them that have the shortest length. And so, the problem to decide whether or not two words define the same point starting from a given point and following the paths that the words label is an important one. This problem is well known as the word problem for groups. It is known to be undecidable in general for finitely generated groups with a finite number of identifying relations, see [19]. Fortunately, in our case, the group is decidable. Indeed, it is the case for most of the Cayley graphs used in geometry. Moreover, in many cases, there is a finite automaton which recognizes whether a word defines a cycle or not. From that, it is easy to devise an automaton which recognizes whether two words define or not the same end point if starting from the same point. Together with another property of groups that goes far beyond the scope of this paper, such groups are called **automatic**. And so, the tilings of the Euclidean plane are Cayley graphs of reflection groups of the Euclidean plane which are automatic. Important works in this line has been done by Epstein, Thurston et al, see [3].

Unfortunately, this situation does not fully extends to the hyperbolic plane.

The first reason is that, in the hyperbolic plane, there are infinitely many regular tilings. This is a consequence of a well known theorem due to Poincaré. But before stating the theorem, we need to remind a few definitions.

Tessellations in the plane – the definition is independent of the geometry that we consider – consist in the following operations. First, take a convex polygon P . Let $\mathcal{S}(P)$ be the set of the lines that support its sides. If \mathcal{E} is a set of polygons, one extends \mathcal{S} to \mathcal{E} by setting that $\mathcal{S}(\mathcal{E}) = \bigcup_{P \in \mathcal{E}} \mathcal{S}(P)$. Given \mathcal{K} a set of lines and \mathcal{E} a set of polygons, we define that $\rho_{\mathcal{K}}(\mathcal{E}) = \bigcup_{k \in \mathcal{K}, Q \in \mathcal{E}} \rho_k(Q)$.

Setting $\mathcal{T}_0 = \{P\}$, we inductively define \mathcal{T}_{k+1} by $\mathcal{T}_{k+1} = \rho_{S(\mathcal{T}_k)}(\mathcal{T}_k)$. Finally, we define $\mathcal{T}^* = \bigcup_{k=0}^{\infty} \mathcal{T}_k$ to be the *tessellation* generated by P . We say that the tessellation is a *tiling* if and only if the following conditions hold:

- any point of the plane belongs to at least one polygon in \mathcal{T}^* ;
- the interiors of the elements of \mathcal{T}^* are pairwise disjoint.

In that definition, lines are defined according to the considered geometry. It may have a consequence on the existence of a tessellation, depending on which polygon is taken in the first step of the construction. As an example, starting from a regular figure, there are three possible tessellations giving rise to a tiling of the Euclidean plane, up to similarities, the three regular tilings which we already know as examples of Cayley graphs.

We can now state the theorem:

THEOREM 1 Poincaré's Theorem, ([20]) – *Any triangle with angles π/ℓ , π/m and π/n such that*

$$\frac{1}{\ell} + \frac{1}{m} + \frac{1}{n} < 1$$

generates a unique tiling by tessellation.

As an immediate corollary of the theorem, tilings based on any regular polygon with p sides and interior angle $\frac{2\pi}{q}$ do exist, provided that $\frac{1}{p} + \frac{1}{q} < \frac{1}{2}$. Such a polygon and the corresponding tiling are denoted by $\{p, q\}$. Now, it is known, see [2] that the Cayley graph of the group generated by the reflections in the sides of the polygon $\{p, 2q\}$ is the tiling $\{2q, p\}$, which is the dual graph of the tiling $\{p, 2q\}$. But the theorem says nothing for tilings $\{s, r\}$ with an odd s . In the example of the pentagrid that we shall later more closely study, *i.e.* the tiling $\{5, 4\}$, it can be shown that this tiling is the Cayley graph of some abstract group but it is not the Cayley graph of any group of isometries of the hyperbolic plane.

4 Locating the tiles in a tessellation of the hyperbolic plane

4.1 The pentagrid

As we already noticed in the previous section, Poincaré's theorem immediately shows that a tiling is generated by tessellation if we take the triangle with the following angles : $\frac{\pi}{5}, \frac{\pi}{4}, \frac{\pi}{2}$. It is easy to see that ten of those triangles share the same vertex corresponding to the angle $\frac{\pi}{5}$ and that such a grouping defines a regular pentagon with right angles. This tiling is classically denoted by $\{5, 4\}$ and we shall from now on call it the **pentagrid**, a representation of which in the south-western quarter of the hyperbolic plane is shown below in Figure 2.

It should be noticed that the pentagrid is the simplest regular grid of the hyperbolic plane. The triangular equilateral grid and the square grid of the Euclidean plane cannot be constructed here as they violate the law about the sum of angles in a triangle which is always less than π in the hyperbolic plane.

Poincaré's theorem was first proved by Henri Poincaré, [20], and other proofs were given later, for example in [1]. In [11], another proof is provided for the existence of the pentagrid which gives rise to a feasible algorithm in order to locate cells. The next section is devoted to a short presentation of that new proof.

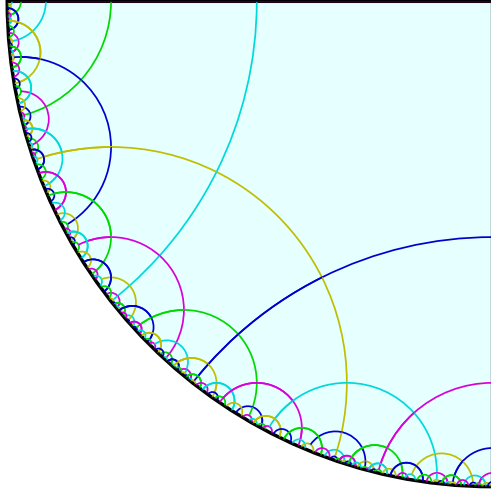


FIGURE 2 *The pentagrid in the south-western quarter*

It is based on a recursive splitting process that is illustrated by Figure 3, below.

The proof given in [11] constructs a bijection between the tiling of the south-western quarter of the hyperbolic plane, say \mathcal{Q} , and a special infinite tree: the *Fibonacci tree*. Notice that \mathcal{Q} is isometric to any quarter of the hyperbolic plane.

Here, we remind sketchily the construction of that bijection.

Let P_0 be the regular rectangular pentagon contained in \mathcal{Q} that has one vertex on the center of the unit disc and two sides supported by the sides of \mathcal{Q} . Say that P_0 is the *leading* pentagon of \mathcal{Q} .

Number the sides of P_0 clockwise by **1**, **2**, **3**, **4** and **5** as indicated below, on Figure 3. As **1** is perpendicular to **2** and **5** and as **4** is perpendicular to **3** and **5**, **2** and **3** do not intersect **5**. The complement of P_0 in \mathcal{Q} can be split into three regions as follows. Line **2** splits \mathcal{Q} into two components, say R_1 and R'_1 with R'_1 containing P_0 . Line **3** splits R'_1 into R_2 and R'_2 with R'_2 containing P_0 . Line **4**

splits R'_2 into P_0 and R_3 . This defines the initial part of a tree: P_0 is associated to the root of the tree, and let us consider that the root has three sons, ordered from left to right and respectively associated to R_3 , R_2 and R_1 . We can denote it as indicated by Figure 3. We shall say that the root is a 3-node because it has three sons.

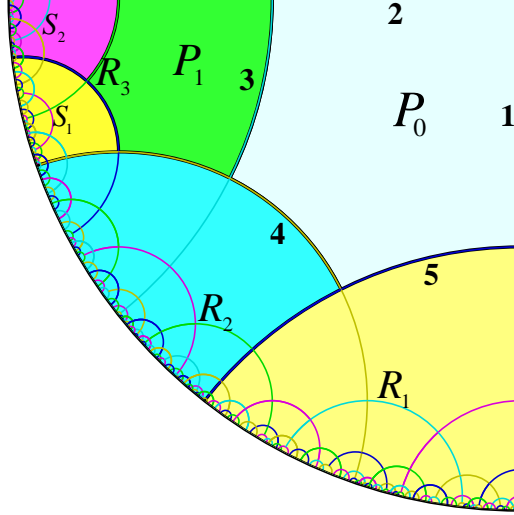


FIGURE 3 *Splitting the quarter into four parts*

First step: regions P_0 , R_1 , R_2 and R_3 , where region R_3 is constituted of regions P_1 , S_1 and S_2 ;

Second step: regions R_1 and R_2 are split as the quarter (not represented) while region R_3 is split into three parts: P_1 , S_1 and S_2 as indicated in the figure.

Regions R_1 and R_2 are isometric images of Q by simple displacements: R_1 is obtained from Q by the displacement along **1** that transforms **5** into **2**. Similarly for R_2 with the displacement along **4** that transforms **5** into **3**. The same splitting into four parts can be repeated for these regions. Their leading pentagons are also 3-nodes.

Now, let us see the status of region R_3 . It is plain that R_3 is *not* isometric to Q , it is a *half-strip*: by analogy with Euclidean geometry, we call here *strip* a region that is delimited by two non-secant lines. Both *half-strips* are delimited by the common perpendicular of the lines. Let P_1 be the reflection of P_0 in **4** with sides which are now numbered anti-clockwise, so that the same number is given to the edges supported by the same h -line. In order to avoid possible confusion, we put the name of the considered pentagon as an index, if needed. Say that P_1 is the leading pentagon of R_3 . Notice that $R_3 \cup P_0$ is transformed into a region \mathcal{S} by the displacement along **5** that transforms $\mathbf{1}_{P_0}$ into $\mathbf{4}_{P_0}$, say Δ , see Figure 3. Define S_1 and S_2 as the respective images of R_2 and R_3 by Δ . Then notice that $\mathcal{S} = S_2 \cup P_1$. Say that S_1 and S_2 are the sons of R_3

and associate also these nodes to their leading pentagon. We say that the node associated to R_3 is a 2-node.

One can clearly see how we may proceed now. Define the following two rules:

- a 3-node has three sons: to left, a 2-node and, in the middle and to right, in both cases, 3-nodes;
- a 2-node has 2 sons: to left a 2-node, to right a 3-node.

Those two rules, combined with the axiom which tells that the root is a 3-node, uniquely define a tree which we call the *standard Fibonacci* tree, see Figure 4, below.

The properties of the standard Fibonacci tree are indicated in [11], [12] and [13], and they are thoroughly proved in [6]. Important works were performed after these pioneer work, they are presented, most of them in full details, in [16, 17, 18]. Here, our attention is focused on on the *location* of the elements of the pentagrid which will allow us to give the tools for Section 6.

4.2 The Fibonacci technology

In principle, the technique that is used in [11, 12] and [13] allows us to find the location of a cell and its neighbours in the pentagrid. This is the reason why the quoted papers assume that the Fibonacci tree is implemented in the hardware of the cellular automaton. A way to implement the tree consists in assuming that the path from the root to each node is known: it may be stored as a sequence of the sides (numbered from 1 to 5) in which reflections are performed starting from the pentagon of the root until the right node is reached. In order to locate the neighbours of the cells in that setting, it can be assumed that for each node, the path to the next node on the same level is also given. Otherwise, it would be possible to compute it, but at the price of a complete induction.

In [6, 8], a new and more efficient way is defined to locate the cells which lie in the quarter, by numbering the nodes of the tree with the help of the positive numbers. We attach 1 to the root and then, the following numbers to its sons, going on on each level from left to right and one level after another one, see Figure 4, below.

That numbering is fixed once and for all in the paper. We fix also a representation of the numbers by means of the Fibonacci sequence, $\{f_i\}_{i \in \mathbb{N}}$, which is defined by the induction relation $f_{n+2} = f_{n+1} + f_n$, and $f_0 = f_1 = 1$.

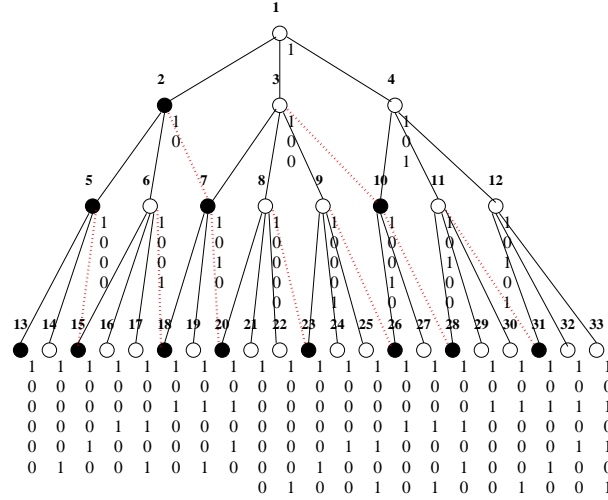


FIGURE 4 The standard Fibonacci tree:

above a node: its number; below: its standard representation.

Notice that the first node of a level has a Fibonacci number with odd index as its number. The number of nodes on a level is also a Fibonacci number. This property is the reason why the tree is called a Fibonacci tree.

It is known that every positive number n is a sum of distinct Fibonacci numbers: $n = \sum_{i=1}^k \alpha_i f_i$ with $\alpha_i \in \{0, 1\}$. Such a representation defines a word $\alpha_k \dots \alpha_1$ which is called a *Fibonacci representation* of n .

It is known that such a representation is not unique, but it can be made unique by adding a condition. Namely, we can assume that in the representation, there is no occurrence of the pattern 11: if $\alpha_i = 1$ in the above word, then $i = k$ or $\alpha_{i+1} = 0$. Following [6, 8], we shall say that this new representation is the *standard* one. In [6, 8], we give a proof of these well-known features.

From the standard representation, which can be computed in linear time from the number itself, see [8], it is possible to find the information that we need to locate the considered node in the tree: we can find its *status*, *i.e.* whether it is a 2-node or a 3-node; the number of its father; the path in the tree that leads from the root to that node; the numbers attached to its neighbours. All this information can be computed in linear time. This is done in great detail in [6] for the considered tree.

In [8], we proved that there are many other Fibonacci trees. There is indeed a continuous family of them.

In order to see that, consider again Figure 3. Indeed, that figure contains all

the information that is needed in order to state the rules that lead to the tree represented in Figure 4.

Now, we can split the quarter in another way, as shown by Figure 5, below.

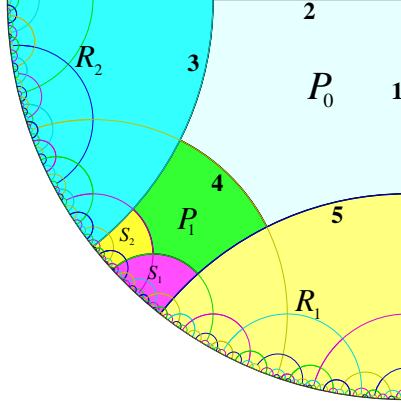


FIGURE 5 *Splitting the quarter into four parts in another way*
Region R_3 consists of P_1 , S_1 and S_2 .

This defines a new splitting which differs from the one defined in [11, 12, 13] and [6], only on the way with which the regions that are isometric to a quarter are chosen.

At this point, we can notice that we can apply the arguments given in [11, 13, 6] in order to prove the bijection between the new tree and the tiling of the quarter. Indeed, when we consider the diameter of a region that tends to zero as the index of the step of splitting tends to infinity, the estimates that we then established are still in force here.

Let us now focus on the trees that are obtained. The standard Fibonacci tree defined in the first papers can be rewritten as indicated in Figure 4 where the numbers of the nodes are also displayed with their standard representation.

The new splitting that we define with the help of Figure 5 gives rise to a new kind of Fibonacci tree, where the rules for the nodes are different for the 3-nodes. In the case of the standard Fibonacci tree, the rules can also be expressed as follows: $\mathbf{2} \rightarrow \mathbf{23}$ and $\mathbf{3} \rightarrow \mathbf{233}$. In the case of this new tree, let us call it *central* Fibonacci tree, the rules are: $\mathbf{2} \rightarrow \mathbf{23}$ and $\mathbf{3} \rightarrow \mathbf{323}$.

As already indicated, the numbering of the nodes in the tree is fixed and so, the standard representation fixes the chosen Fibonacci representation. However, the algorithms which gives the status of a node, the number of the father, the path from the root to the considered node and the numbers of its neighbours will be different, see [7, 8] for more details.

There are infinitely many general Fibonacci trees. They can be all constructed by a random algorithm using a dice¹ as follows:

- construct the root as a 3 node, which is at level 0;
- iteratively construct levels one after another:
 - for each node of the current level:
 - throw the dice and let r be the result
 - for a 2-node apply rule $\mathbf{2} \rightarrow \mathbf{23}$ iff $r < 4$, otherwise $\mathbf{2} \rightarrow \mathbf{32}$
 - for a 3-node apply rule $\mathbf{3} \rightarrow \mathbf{232}$ iff $r < 3$, else $\mathbf{3} \rightarrow \mathbf{323}$ if $r < 5$, otherwise $\mathbf{3} \rightarrow \mathbf{332}$.

As we have only permutations in the position of the 2-node among the sons of a node, this does not change the number of nodes which occur and, by induction on the level of the considered tree, it is easy to see that the number of nodes in a considered level is always the same for any general Fibonacci tree. Consequently, the numbering is always the same and, hence the standard representation attached to the numbers of the nodes only depends on the depth of the node in the tree, and on its rank on its level.

If $a_k \dots a_1 a_0$ is the standard representation of n , say that n ends in $\alpha_1 \alpha_0$.

Following [8], call *continuator* of a node n with $a_k \dots a_1 a_0$ as its standard representation the node whose standard representation is $a_k \dots a_1 a_0 00$. In the case of the standard Fibonacci tree, the continuator of a node is always one of its sons and in that case, it is called the *preferred son*. In [8], we noticed that in general the continuator of a node is not necessarily among the sons of the node. There are trees in which for some nodes the continuator is not among the sons and in the same trees, there are also nodes that contain two continuators of nodes among their sons. These properties are thoroughly studied in [8] where we show that there is a continuous number of Fibonacci tree that possess the preferred son property for every node. If n is a node, denote by $c(n)$ its continuator. We shall denote by c^{-1} the converse operation: $c^{-1}(n)$ is the node with $a_k \dots a_2$ as its standard representation where $a_k \dots a_1 a_0$ is the standard representation of n . Then, in the standard Fibonacci tree, the neighbours of a node n are:

- if n is a 2-node which ends in 00:

$$c^{-1}(n), c^{-1}(n)-1, c(n), c(n)+1, c(n)+2$$
- if n is a 2-node which ends in 10:

$$c^{-1}(n)+1, c^{-1}(n), c(n), c(n)+1, c(n)+2$$
- if n is a 3-node:

$$c^{-1}(n), c(n)-1, c(n), c(n)+1, c(n)+2$$

where the neighbours are indicated in the anticlockwise way.

The path from the root to a given node is obtained by repeatedly applying the c^{-1} operation with a correction for 2-nodes that end in 10, starting the process from the node and then taking the mirror of that list of nodes.

¹We use a *cubic*, hence Euclidean, dice in a three-dimensional Euclidean space.

4.3 Implementation issues

We consider now implementation issues.

For that questions, we need to take the Fibonacci tree that will give us the fastest algorithms that can solve the location problem. As an example, in the case of the standard Fibonacci tree, the algorithms are linear, but as shown in [8], for another tree, the algorithms are still linear, but a bit faster.

The reason of our choice is that in the case of the standard Fibonacci tree, finding the *status* of a node n is not immediate from the standard representation of n . The status is 2 when the last 2 digits are 10 and it is 3 when the last 2 digits are 01, but when it is 00, we have also to look at the last two digits of the standard representation of node $n-1$: if it is 10, n is a 3-node, if it is 01, n is a 2-node. The algorithm for the neighbours is rather simple but it relies on the determination of the status.

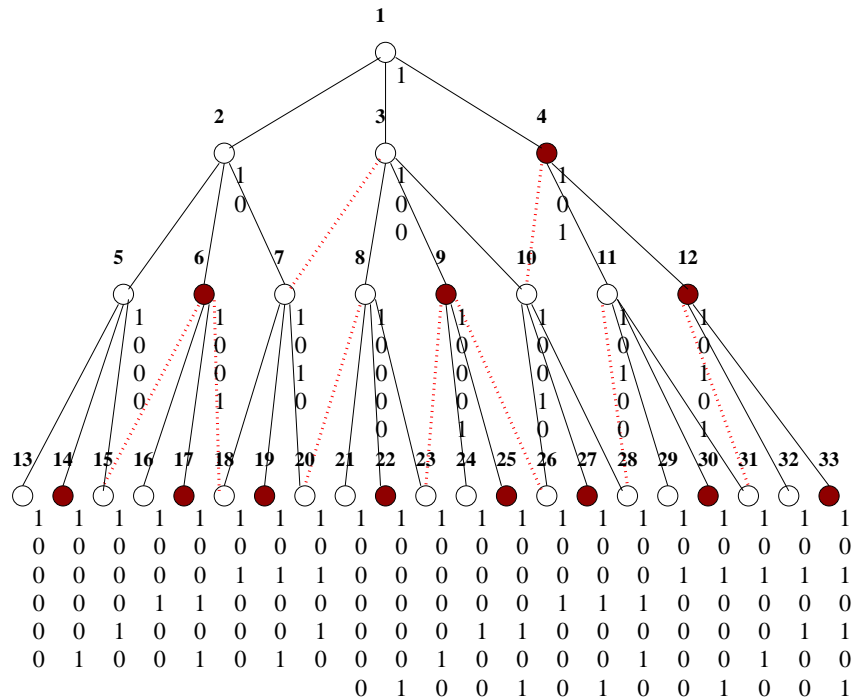


FIGURE 6 *The best Fibonacci tree:
above a node: its number; below: its standard representation.*

As indicated in [8] there is a Fibonacci tree such that its 2-nodes are exactly the nodes whose standard representation ends with 01. This tree possesses the preferred son property and so, the algorithm for the path and for the neigh-

bours are linear too. For the path, the algorithm is simpler as for the standard Fibonacci tree because the father of a node is always c^{-1} , the root and node 2 being excepted. For the neighbours, we have here the rules:

if n is a 3-node that ends in 10:
 $c^{-1}(n), c(n), c(n)+1, c(n)+2, c^{-1}(n)+1$
 if n is a 2-node (it ends in 01) or if it is a 3-node that ends in 00 for which $c^{-1}(n)$ is a 3-node:
 $c^{-1}(n), c(n)-1, c(n), c(n)+1, c(n)+2$
 otherwise (n is a 3-node that ends in 00 for which $c^{-1}(n)$ is a 2-node):
 $c^{-1}(n), c^{-1}(n)-1, c(n), c(n)+1, c(n)+2$

We notice that there are indeed three possible configurations: for nodes in 01 and nodes in 00 whose the father is in 00 or 01, for nodes in 10 and for nodes in 00 whose father is in 10, see Figure 6, below.

Notice that besides the root for which the rule of the son is **3** \rightarrow **332**, for all other nodes the rules are **2** \rightarrow **32** for 2-nodes and **3** \rightarrow **323**.

According to this information, we can fix the format of the local rules for cellular automata in the pentagrid.

First, we have to remark that the numbering of the nodes must be considered as a hardware feature. In the Euclidean case, the same convention is done but in that case the coordinate system is so evident that this fact is usually unnoticed. However, implementation programs have to fix such a system.

Taking into account the considerations that we just developed, we can also consider that the notions of father, of sons, of preferred son is also a hardware feature. We express these properties when we say that any cell *knows* which one is its father, what are the numbers of its neighbours, what is its status and so on for similar questions.

This allows us to consider only *states* of the automaton and to give a uniform description. The format of the rules will be the following:

<i>fa</i>	<i>n1</i>	<i>n2</i>	<i>n3</i>	<i>n4</i>	<i>old</i>	\rightarrow	<i>new</i>
-----------	-----------	-----------	-----------	-----------	------------	---------------	------------

where *fa* is the state of the father of the cell and *n1*, *n2*, *n3* and *n4* are the states of the other neighbours of the cell, listed in an anticlockwise way starting from the father. Of course, *old* is the current state of the cell and *new* is the state that it receives from the application of the local rule.

5 An application to tiling problems

The location technique that we give in sub-section 4.2. of this paper, also allows us to solve some tiling problems in the hyperbolic plane.

In [9], one studies the tilings that can be generated by replication of a single pentagon with coloured side, in such a way that the colours of the sides do match and by using only displacements along the sides of the tessellation. There are

at most five colours that are denoted by 1, 2, 3, 4 and 5. The question that is addressed by the paper is the following. If we give the number of colours and the assortment of the colours on the sides of the initial pentagon, how many tilings can be generated under the above restrictions? The answer is surprisingly not as trivial as it is in the Euclidean case with a square.

A basic remark is to notice that the displacements along the lines of the tiling give for free the rotations that leave the tiling globally invariant. This allows us to reduce the number of cases to be investigated and to consider the assortments of colours up to circular permutations.

THEOREM 2 (Margenstern) – *The number of possible tilings with a single pentagonal tile on the pentagrid with the assortments of j colours, $1 \leq j \leq 5$ and satisfying the condition of displacements only along the lines of the pentagrid are given by Table 1.*

TABLE 1 Table of the results of theorem 2

5	1 2 3 4 5	no solution		1 2 3 1 2	no solution
4	1 1 2 3 4	2 solutions		1 2 3 1 3	no solution
	1 2 1 3 4	no solution	2	1 1 1 1 2	2^{\aleph_0} solutions
3	1 1 1 2 3	2^{\aleph_0} solutions		1 1 1 2 2	2^{\aleph_0} solutions
	1 1 2 1 3	2^{\aleph_0} solutions		1 1 2 1 2	2^{\aleph_0} solutions
	1 1 2 2 3	4 solutions	1	1 1 1 1 1	1 solution
	1 1 2 3 2	2^{\aleph_0} solutions			

In the case of the assortment $\boxed{1\ 1\ 1\ 1\ 2}$ where there is a continuous number of solutions, Figure 7 illustrates two cases.

Consider the picture (a) of that figure. It gives an example from that family of tilings. The construction starts from the standard Fibonacci tree, where all 2-nodes are on a same line starting from some initial node which is a 3-node, among them the root. On that line, the side to the father is coloured with 2 for each two nodes. In the figure, we make use of the same colour for a line of 2-nodes that are connected in that way, the starting point of the line being a 3-node. We make use of 3 colours in order that the phenomenon should become clear.

Now, if we randomly apply the rules used to define the succession of 2-nodes, namely the rules $2 \rightarrow 2\ 3$ and $2 \rightarrow 3\ 2$, we obtain a continuous family of tilings.

We consider also another possibility which is given by the picture (b) of Figure 7. In this picture, pentagons are all linked together along their single side that is coloured by 2. We can do a bit more: this association of pairs, which

gives rise to rectangular (non-regular) hexagons, can be performed in such a way that each vertex is shared by exactly three hexagons.

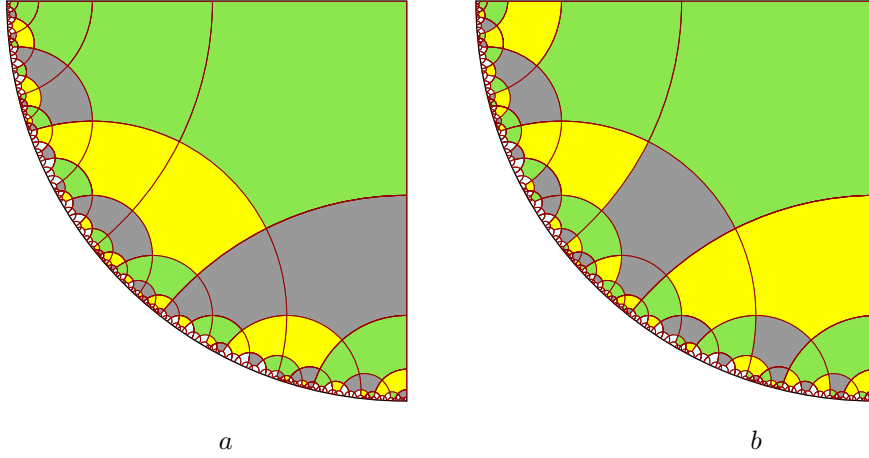


FIGURE 7 *Two tilings with colouring*

1	1	1	1	2
---	---	---	---	---

.

We turn now to the Cayley graph problem that we announced in section 3.

In [10], we show that the pentagrid is not the Cayley graph of a sub-group of the isometries of the hyperbolic plane. The proof is by cases: we show first that there should be at least one displacement. We easily rule out the case when all the sides of a pentagon represent displacements. And so, there is an even number of products of three reflections, they are called *glides*, and at least one displacement. The different cases are eliminated by considering a pair of independent vectors on one vertex of the pentagon and on looking at the result of five isometries whose product should be the identity, which is neither the case.

However, the pentagrid is the Cayley graph of an abstract group. To see that point, notice that if all generators that label the arcs from a vertex are involutions, *i.e.* $g^2 = 1$ for all those generators g , the existence of the group boils down to the following tiling problem. We have at our disposal four colours, 1, 2 3 and 4 and we have to colour the sides of all pentagons of the grid in such a way that at any vertex, all the colours are present on the sides that meet in the vertex. This can be performed by using the standard Fibonacci tree and proving by induction on the depth and on the rank in a level that the process goes endlessly with success.

6 About automaticity or not of groups on hyperbolic tilings

6.1 The case of the pentagrid and of the heptagrid

THEOREM 3 (Gasperin-Margenstern) *Any group having the pentagrid or the heptagrid as a Cayley graph is not automatic.*

Proof of the theorem. The idea of the proof consists in looking at a family of closed paths in each of these tilings which cannot be recognized by a finite automaton. We remind the reader that a **path** is a finite set of tiles T_0, \dots, T_n such that for $i \in \{0 \dots n-1\}$, T_i and T_{i+1} share a common side. We say that the **length** of the path is n and that the path is **closed** if $T_0 = T_n$.

The family of paths we consider is the set of paths P_n defined as follows. The path starts from the leftmost son G of the root F of a Fibonacci tree \mathcal{F} of the tiling. Call \mathcal{B} the subtree of \mathcal{F} rooted at G . Then, the follows the leftmost branch λ of \mathcal{B} until its level n . There, it follows the level n until it meets the branch ρ of \mathcal{B} which is the rightmost branch of this tree. Then, when the path reaches ρ , it goes back to the root of \mathcal{B} by following ρ .

Assume that a group corresponding to the tiling is automatic. There is a finite automaton \mathcal{A} such that \mathcal{A} recognizes the paths of the tiling which are closed and rejects those which are not closed. Let Q be the set of states of \mathcal{A} and let $N = |Q|$, the number of elements of Q . Let B be the finite set of symbols attached to each tile of the tiling and let $r = |B|$.

It is plain that \mathcal{A} accepts all P_n 's. Consider a run of the automaton on $P_{r.N+2}$. Looking at the couples (α, q) read on the tiles of path which are on λ , where α is the symbol attached to the tile and q is the state of \mathcal{A} when it reads this tile, necessarily there are two tiles on the restriction of the path to λ on which the couple (α, q) are the same. Let T_i and T_j be these tiles of $P_{r.N+2}$. Then, the subpath from T_{i+1} up to T_j can be appended as many time as we wish in between T_j and T_{j+1} . Let $k = j-i$ and let m be the number of iterations of the subpath from T_{i+1} up to T_j . Let $Q_{r.N+2,k,m}$ be the new path: appending the subpath from T_{i+1} up to T_j boils down to apply the translation τ which transforms T_j into T_{i+km} to the tiles of $P_{r.N+2}$ from T_j up to T_n . The translation is correctly defined since by construction there exists a copy of the tree we move. As $P_{r.N+2}$ goes back to G and as \mathcal{B} is globally unchanged by the translation τ , $Q_{r.N+2,k,m}$ goes back to the image of G by τ : this image is not G , the root of \mathcal{B} . Now, the automaton also recognizes $Q_{r.N+2,k,m}$, a contradiction as $Q_{r.N+2,k,m}$ is not closed. \square

COROLLARY 1 *There are infinitely many groups with Cayley graph corresponding to tessellations of the hyperbolic plane which are not hyperbolic.*

Proof. This argument can be repeated for all tessellations $\{p, 4\}$ with $p \geq 5$ and all tessellations $\{p, 3\}$ with $p \geq 7$ as the tessellations $\{p, 4\}$ and $\{p+2, 3\}$ are generated by the same tree which generalizes the Fibonacci tree. \square

Note that we have the following result, which may have a connection with Theorem 3:

THEOREM 4 (Margenstern, [10]) *The pentagrid is not the Cayley graph of a group of isometries leaving the pentagrid globally invariant.*

We repeat the proof of [10] for the convenience of the reader. We use Figure 8, which is a bit different from the figure used in [10].

Proof. Assume that the pentagrid is the Cayley graph of a group G of isometries which leave the pentagrid globally invariant: any pentagon of the tiling is transformed into a pentagon of the tiling and the mapping is bijective. As we have four edges at any vertex, G has four generators g_1, g_2, g_3 and g_4 .

Consider a pentagon P_0 whose vertices are denoted A, B, C, D and E , in this order while clockwise turning around the tile, see Figure 8. We may decide that P_0 is the leading pentagon of a sector of the pentagrid. We give it number 1 and the pentagons 2, 3 and 4 are, by construction, those defined by the reflection of P_0 in the sides ED, DC and CB respectively. In the figures, we indicate the numbering for a few pentagons which allows us to easily derive all the numbers of the pentagons we shall consider in the proof.

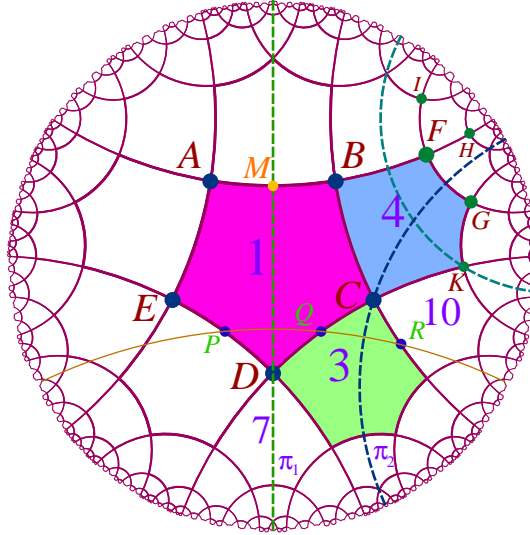


FIGURE 8 The picture for the proof of Theorem 4.

We also know that, as in the Euclidean case, the products of reflections in lines which do not yield the identity can be reduced to three kinds of transformations: one reflection, two reflections or three reflections. And so we shall speak of odd and even motions, the even motions being exactly those which can be reduced to a product of two reflections in lines. The even motions are characterized by the intersection property of the axes of the reflections which

define the motion: rotation, if the axes meet in the plane, ideal rotation, if the axes are parallel, shift along the common perpendicular of the axes when they are non-secant.

We may assume that g_1 transforms A into B and we may assume that g_1 is an even motion: if all g_i 's are all odd motions, a product of an odd number of them will remain odd and thus, cannot yield the identity. Let F be the image of A under the reflection in B . Let G, H and I be the other vertices of the edges of pentagons which about B . If g_1 transforms F into B , then the intersection of the lines π_1 and π_2 the respective perpendicular of AB and FB tells us about the nature of g_1 . Now, as π_1 and π_2 have a common perpendicular, they are non-secant. Moreover, as g_1 is a shift, the common perpendicular is the axis of the shift: the line which is globally invariant under the shift. And so, g_1 is the shift along AB which transforms A into B . We have the same conclusion, for a very similar reason if g_1 transforms F into H .

Now, g_1 may also transform F into G or I instead of transforming it into B or H . We may look at the case of G as the case of I is very similar by reflection in AB . Again, we consider the intersection of π_1 with π_2 where π_2 is now the perpendicular bisector of FG . Let M be the midpoint of AB . Clearly, the triangles DBC and DAE are equal from which we conclude that the triangle ABD is isosceles with AB as its basis and from this, we easily conclude that MD is also the perpendicular bisector of AB so that $\pi_1 = MD$. From the equalities of angles at D we derive from this property, we conclude that if P and Q are the mid-points of ED and DC respectively, π_1 is also the perpendicular bisector of PQ . If we consider the perpendicular bisector of FG , the just performed argument shows that π_2 passes through C and through N the mid-point of FG . It is also not difficult to prove that if R denotes the mid-point of the side of pentagon 10 which has C as a vertex and which is not shared by pentagon 4, then the triangle CQR is equal to the triangle DQP . From the previous study on pentagon 1 transported to pentagon 4, we know that the reflection of CQR in C is an isosceles triangle whose basis is the image of QR and the perpendicular bisector of the image of the basis is π_2 . Now, by the properties of the angles at C which are those of the angles at D , we notice that π_2 is globally invariant under the reflection in C . Accordingly, π_2 is perpendicular to QR . Now, from the equality of the triangles CQR and DQP , it is not difficult to prove that the points P, Q and R lie on the same line. Accordingly, π_1 and π_2 also have a common perpendicular in this case and so g_1 is again a shift. Now, the line which is globally invariant under the shift g_1 is the line PQR . Now, it is easy to show that the image of P under this shift, as it globally preserves the tiling, should be at least R , as we have to consider the half-plane defined by AE which contains B , but is in this case, the image of A is K and so, it cannot be B .

And so, if g_1 is an even motion, it must be the shift along AB which transforms A into B . Now, if all g_i 's are even motions, they are shifts along sides of a pentagon which transform a vertex supported by the axis of the shift to the other vertex of the side. Now, we can assume that we have five shifts $g_{i_1}, g_{i_2}, g_{i_3}, g_{i_4}$ and g_{i_5} such that g_{i_1} transforms A into B , g_{i_2} transforms B into C , g_{i_3} transforms C into D , g_{i_4} transforms D into E and g_{i_5} transforms E into A . Now,

considering the angle (BA, BC) , which is inside pentagon 1, it is not difficult to see that this angle is transformed into (BC, BF) by $g_{i_1} \circ g_{i_2} \circ g_{i_3} \circ g_{i_4} \circ g_{i_5}$, an angle which is outside pentagon 1, so that this product cannot be the identity.

The conclusion is that if $g_{i_1} \circ g_{i_2} \circ g_{i_3} \circ g_{i_4} \circ g_{i_5} = 1$ there are exactly two or exactly four distinct g_i 's that are odd motions of reflections in line. But the case of four distinct g_i 's which are all odd motions has already been ruled out. And so, two g_i 's are odd motions and two g_i 's are shifts.

We may assume that g_1 and g_2 are the two generators which are odd motions. And so g_1 is a reflection in a line or a product of three reflections in lines. This latter situation is that of a glide and it can be shown that a glide can be assumed to be in the form $\rho_\ell \circ \rho_a \circ \rho_b$ where a, b are non-secant and ℓ is the common perpendicular of a and b . Consider P_0 a pentagon and assume that g_1 is a glide transforming A , a vertex of P_0 into B the other vertex of an edge c of P_0 . Now, consider $\gamma = \rho_c \circ g_1$. It is a product of an even number of reflection of lines and so, γ can be reduced to an even motion. From what we have seen, it is the shift along c transforming A into B . And so, the glide is necessarily a reflection in an edge of a pentagon followed by a shift along the same edge. Note that in fact, the product of the reflection and the shift are here commutative as they have the same axis.

Note that if g_1 is a single reflection in a line, as it transforms A into B it is the reflection in π_1 . In all cases, we shall say that AB is the side defining g_1 .

g_1	g_2		g_1	g_2	
g	g	2	g	g	4
g	r	4	g	r	2
r	g	4	r	g	2
r	r	2	r	r	4

TABLE 2 Showing that $g_{i_1} \circ g_{i_2} \circ g_{i_3} \circ g_{i_4} \circ g_{i_5}$ is not the identity. To left, the sides defining g_1 and g_2 are contiguous. To right, the defining sides are separated by one side of the pentagon. In all cases, the starting angle is 1.

Now, consider the second odd motion g_2 . There are two cases, depending whether the side which defines g_2 is contiguous to that of g_1 or not. If it is not the case, we may assume that the side defining g_2 is CD by symmetry of the pentagon. If g_2 is defined by BC , we have four cases, depending on the type of odd motions we have for g_1 and g_2 . We also have four cases if g_2 is defined by CD . We can indicate the results by Table 2 where we denoted the four angles around B as 1, 2, 3 and 4, 1 being the angle (BA, BC) and the numbers being increasing while clockwise turning around the vertex. The nature of the odd motion is indicated by the letters r and g for reflection in a line and glide respectively. We always start from angle 1 and look at the result when applying $g_{i_1} \circ g_{i_2} \circ g_{i_3} \circ g_{i_4} \circ g_{i_5}$ where $g_{i_1} = g_1$. We can see in Table 2 that the result is never angle 1. Accordingly, Theorem 4 is proved. \square

However, if we remove the condition that the group should be a sub-group of the group of isomorphisms which leaves the tiling globally invariant, then it

is possible to represent the pentagrid in this way as the following result states.

THEOREM 5 (Margenstern, [10]) *The pentagrid is the Cayley graph of some abstract group.*

Proof. Assume that there is a finitely generated group G which is generated by four elements x such that $x^2 = 1$ for each of these elements and such that the pentagrid is the Cayley graph of G .

This is equivalent to the following condition. There is an assignment of each side of the pentagons of the pentagrid onto a set of four colours S such that: any edge belonging to two neighbouring pentagons receive the same assignment in both pentagons and that at every vertex, the sides abutting the vertex are coloured with all the colours of S .

We shall see that we can tile the pentagrid under these constraints to which we append a new one. Denote the four colours by **a**, **b**, **c** and **d**. While counter-clockwise turning around a tile, putting the colours into a word yields what we call a **contour word** of the tile. Note that the contour word is not unique: the different ones are obtained from each other by an appropriate circular permutation. We define an α -tile with $\alpha \in \{\mathbf{a}, \mathbf{b}, \mathbf{c}\}$ as a tile whose contour word is $d\beta\gamma\beta\gamma$ with $\{\alpha, \beta, \gamma\} = \{\mathbf{a}, \mathbf{b}, \mathbf{c}\}$. We shall see that we can tile the pentagrid by α -tiles only with $\alpha \in \{\mathbf{a}, \mathbf{b}, \mathbf{c}\}$ and with observing the constraint that all colours abut at each vertex.

Let us fix a central tile C . Let us put a c -tile at it. We shall denote its contour word as $d\alpha\beta\alpha\beta$ with $\{\alpha, \beta\} = \{\mathbf{a}, \mathbf{b}\}$. Now, we can see that the five roots of Fibonacci trees surrounding C can be denoted as follows:

at d	$d\alpha\beta\alpha\beta$
at α	$\alpha\gamma\alpha\gamma d$
at β	$\beta\gamma\beta\gamma d$
at α	$\alpha\gamma\alpha\gamma d$
at β	$\beta\gamma\beta d\gamma$

where the first letter of the contour word corresponds to the side shared with C . This dispatching of the tiles is illustrated by Figure 9.

Note that the nodes at α and the first one at β can be considered of the same type $\alpha\beta\alpha\beta d$ as the letter d is always in the last position. We can define the **type** of a node ν as the position of d among its neighbours, the father of ν being its neighbour 1 and numbering the other neighbours increasingly by counter-clockwise turning around ν . We can see that, around the central node, we can decide that three consecutive nodes have type 5, one of the others having type 1 by construction: necessarily this node is before the group of nodes with type 5 while counter-clockwise turning around the central tile. It is not difficult to see that the other one has type 4.

In order to avoid complicate figures on which not much is visible, we shall represent the colours of a tile as follows: $\frac{1}{2\ 3\ 4\ 5}$ for the white nodes and

$\frac{2\ 1}{3\ 4\ 5}$ for the black ones, where in place of the numbers we put the colour

associated to the side with this number. We remind the reader that 1 is the side shared with the father and that the numbers are increasing while counter-clockwise turning around the tile. We call this representation **colour pattern**. Accordingly, the colour patterns of the neighbours of the central cell are:

$$\begin{array}{cccccc} \underline{\mathbf{d}} & \underline{\alpha} & \underline{\beta} & \underline{\alpha} & \underline{\beta} & \underline{\mathbf{d}} \\ \alpha \beta \alpha \beta & \gamma \alpha \gamma \mathbf{d} & \gamma \beta \gamma \mathbf{d} & \gamma \alpha \gamma \mathbf{d} & \gamma \beta \mathbf{d} \gamma & \alpha \beta \alpha \beta, \end{array}$$

where the types are 1, 5, 5, 5, 4 and 1 respectively, the first tile being repeated after the last one in order to make the vertices in between four tiles all visible while turning around the central cell. Here and in our sequel, we use α , β and γ as variables with the condition that $\{\alpha, \beta, \gamma\} = \{\mathbf{a}, \mathbf{b}, \mathbf{c}\}$. Later, when black nodes also will appear, we shall append the mention of the status of the node together with its type, as an example 1_b for a black node of type 1. If we consider two consecutive tiles, the two rightmost letters of the left-hand side tile, taking into account both lines of the colour pattern, and the two leftmost letters of the right-hand side represent sides sharing a common vertex. Now we note that at each vertex of tiles sharing a vertex, the four letters, \mathbf{a} , \mathbf{b} , \mathbf{c} and \mathbf{d} are present. Now, looking at the above tiles, it can be seen that when \mathbf{d} is on a side shared by a son of a node, for this son, \mathbf{d} appears on side 1. We shall see that for the other sons, we can decide that \mathbf{d} appears on side 2. Next, for nodes of type 2, we shall see that most sons we can decide that \mathbf{d} will appear on side 5. More rarely, types 4 and 3 will also appear.

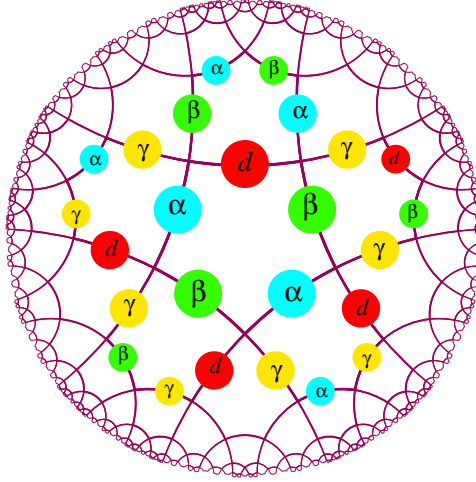


FIGURE 9 *The distribution of α -tiles around the central cell.*

Let us now see the checking steps. They are structured in the same way: the configuration, according to the pattern mentioned in Table 3, and then developed by using the schemes above defined. There will be colours which can be defined by variables only with conditions in order to preserve the presence

of exactly the four colours at any vertex. We then study the configuration for each son of the considered nodes and we shall summarize this in a way again used in Table 3 which gathers all results obtained in the discussion.

Configuration: 5 5

For the right-hand side node, all its neighbours i with $i \in \{2..5\}$ can be assigned the type 2. Indeed, we have $\frac{\alpha}{x \alpha x \mathbf{d}}$ $\frac{\beta}{\gamma \beta \gamma \mathbf{d}}$, and now we can derive:

$$\frac{\cdot x}{\cdot \cdot y} \quad \frac{\alpha}{\mathbf{d} y \alpha y} \quad \frac{x}{\mathbf{d} y x y} \quad \frac{\mathbf{d} \gamma}{\alpha \gamma \alpha} \quad \frac{\beta}{\mathbf{d} \alpha \beta \alpha} \quad \frac{\gamma}{\mathbf{d} u \gamma u} \quad \frac{\mathbf{d} \cdot}{v \cdot v}$$

where $\{x, y\} = \{\beta, \gamma\}$ and $\{u, v\} = \{\alpha, \beta\}$. As can be seen, all nodes but the first son are of type 2. For the first node, its type is in $\{2..4\}$, depending on the left-hand side node with respect to the node of type 5: $\frac{\alpha}{x \alpha x \mathbf{d}}$.

We complete the situation of the neighbours of the central tile by considering the two sequences: 5, 4 and also 4, 1, 5.

Configuration: 5 4

We have: $\frac{\alpha}{\gamma \alpha \gamma \mathbf{d}}$ $\frac{\beta}{\gamma \beta \mathbf{d} \gamma}$, which gives us:

$$\frac{\cdot \gamma}{\cdot \cdot \beta} \quad \frac{\alpha}{\mathbf{d} \beta \alpha \beta} \quad \frac{\gamma}{\mathbf{d} \beta \gamma \beta} \quad \frac{\mathbf{d} \gamma}{\alpha \gamma \alpha} \quad \frac{\beta}{\mathbf{d} u \beta u} \quad \frac{\mathbf{d}}{v \beta v \beta} \quad \frac{\gamma \alpha}{\alpha \gamma \mathbf{d}}$$

where $\{u, v\} = \{\alpha, \gamma\}$.

We can summarize these relations by writing the types of the nodes in the following way: $\frac{5}{x - 2 \quad 2 \bullet 2} \quad \frac{4}{2 - 2 \quad 1 \bullet 5}$. The dash is put in between the black son and the white ones of the same node, the \bullet is put between the last son of a node ν and the first son of ν . Also note that the same black node appears twice in the above scheme: once as the fifth neighbour of a node of type 5 and the second time as the first son of a node of type 4.

Configuration: 4 1 5

We have:

$$\frac{\beta}{\gamma \beta \mathbf{d} \gamma} \quad \frac{\mathbf{d}}{\alpha \beta \alpha \beta} \quad \frac{\beta}{\gamma \beta \mathbf{d} \gamma} \cdot \quad \frac{\alpha}{\gamma \alpha \gamma \mathbf{d}}$$

Taking into account what we have found for 5 and 4, we can now derive:

$$\frac{\gamma \alpha}{\alpha \gamma \mathbf{d}} \quad \frac{\beta}{\gamma \beta \gamma \mathbf{d}} \quad \frac{\alpha}{\gamma \alpha \gamma \mathbf{d}} \quad \frac{\beta \gamma}{\gamma \mathbf{d} \beta} \quad \frac{\alpha}{\mathbf{d} \beta \alpha \beta} \quad \frac{\gamma}{\mathbf{d} x \gamma x} \quad \frac{\mathbf{d} \cdot}{y \mathbf{d} \beta}$$

with $\{x, y\} = \{\alpha, \beta\}$. This information can be rewritten as:

$$\frac{4}{x - 2 \quad 1 \bullet 5} \quad \frac{1}{5 - 5 \quad 5 \bullet 4} \quad \frac{5}{4 - 2 \quad 2 \bullet 2}.$$

Note the node of type 4 which appears here is a black node.

At this step, several new patterns have to be analyzed: $2\ 2\ 2_b$, $2_b\ 2\ 1$, $2\ 1\ 5_b$, $5_b\ 5$ and $5\ 4_b\ 2$.

Configuration: $2\ 2\ 2_b$

Accordingly, we consider the following situation: $\frac{\alpha}{\mathbf{d}\ \gamma\ \alpha\ \gamma} \quad \frac{\beta}{\mathbf{d}\ \gamma\ \beta\ \gamma} \quad \frac{\alpha\ \mathbf{d}}{\dots}$.

It is not difficult to check that this time we obtain:

$\frac{\cdot\ \mathbf{d}}{z\ \cdot\ z} \quad \frac{\gamma}{y\ \gamma\ y\ \mathbf{d}} \quad \frac{\alpha}{\beta\ \alpha\ \beta\ \mathbf{d}} \quad \frac{\gamma\ \mathbf{d}}{\beta\ \gamma\ \beta} \quad \frac{\gamma}{\alpha\ \gamma\ \alpha\ \mathbf{d}} \quad \frac{\beta}{\alpha\ \beta\ \alpha\ \mathbf{d}} \quad \frac{\gamma\ \alpha}{\alpha\ \gamma\ \mathbf{d}} \quad \frac{x}{u\ x\ u\ \mathbf{d}}$
with $\{y, z\} = \{\alpha, \beta\}$ and $\{u, x\} = \{\beta, \gamma\}$. We can summarize these results as

$$\frac{2}{1 - 5\ 5 \bullet 1} \quad \frac{2}{1 - 5\ 5 \bullet 5} \quad \frac{2}{5 - 5 \bullet x}$$

Configuration: $2_b\ 2\ 1$

The nodes are given by the following patterns: $\frac{\mathbf{d}\ \alpha}{\gamma\ \alpha\ \gamma}$, $\frac{\beta}{\mathbf{d}\ u\ \beta\ u}$ and $\frac{\mathbf{d}}{x\ v\ x\ v}$, with $\{u, x\} = \{\alpha, \gamma\}$ and $\{v, w, x\} = \{\alpha, \beta, \gamma\}$. Using what we have seen for 1 with $4\ 1\ 5$, the computation yields:

$\frac{\cdot\ \gamma}{\gamma\ \cdot\ \mathbf{d}} \quad \frac{\alpha}{\beta\ \alpha\ \gamma\ \mathbf{d}} \quad \frac{\gamma\ \mathbf{d}}{\beta\ \gamma\ \beta} \quad \frac{u}{x\ u\ x\ \mathbf{d}} \quad \frac{\beta}{x\ \beta\ x\ \mathbf{d}} \quad \frac{u\ x}{x\ u\ \mathbf{d}} \quad \frac{v}{w\ v\ w\ \mathbf{d}}$
with $\{u, x\} = \{\alpha, \gamma\}$ and $\{v, w, x\} = \{\alpha, \beta, \gamma\}$. A possible assignment of the variables is $x = \alpha$, $v = \beta$ and $u = w = \gamma$. This can be summarized as:

$$\frac{2}{5 - 5 \bullet 1} \quad \frac{2}{1 - 5\ 5 \bullet 5} \quad \frac{1}{5 - 5\ 5 \bullet x}$$

Note, that in $4\ 1\ 5$, the last node of 1 is 4 and here, it is not determined.

Configuration: $2\ 1\ 5_b$

This means that the nodes we consider are $\frac{\alpha}{\mathbf{d}\ x\ \alpha\ x}$, $\frac{\mathbf{d}}{y\ z\ y\ z}$ and $\frac{\beta\ t}{t\ \beta\ \mathbf{d}}$, with $\{x, y\} = \{\beta, \gamma\}$ and $\{t, z\} = \{\alpha, \gamma\}$. As an example, $y = t = \gamma$, $x = \beta$ and $z = \alpha$ are possible choices. Without repeating previous results for the sons of a node of type 2, computations yield:

$\frac{\alpha}{\beta\ \alpha\ \beta\ \mathbf{d}} \quad \frac{\gamma\ \beta}{\beta\ \gamma\ \mathbf{d}} \quad \frac{z}{w\ z\ w\ \mathbf{d}} \quad \frac{\beta}{w\ \beta\ w\ \mathbf{d}} \quad \frac{z\ w}{w\ z\ \mathbf{d}} \quad \frac{\beta}{z\ \beta\ \mathbf{d}\ z}$
with $\{u, v\} = \{\alpha, \beta\}$ and $\{w, z\} = \{\alpha, \gamma\}$. This gives us:

$$\frac{2}{1 - 5\ 5 \bullet 5} \quad \frac{1}{5 - 5\ 5 \bullet 5} \quad \frac{5}{5 - 4 \bullet 2}$$

Configuration: 5_b 5

It is very similar to the case 5 5. We have: $\frac{x \beta}{\beta x \mathbf{d}} \quad \frac{\alpha}{\gamma \alpha \gamma \mathbf{d}}$, with $x \in \{\alpha, \gamma\}$. Computations give us:

$$\frac{\cdot \beta}{\cdot \cdot y} \quad \frac{x}{\mathbf{d} y x y} \quad \frac{\mathbf{d} \gamma}{\beta \gamma \beta} \quad \frac{\alpha}{\mathbf{d} \beta \alpha \beta} \quad \frac{\gamma}{\mathbf{d} u \gamma u} \quad \frac{\mathbf{d} \cdot}{v \cdot \cdot}$$

with $\{x, y\} = \{\alpha, \gamma\}$ and $\{u, v\} = \{\alpha, \beta\}$. This can be summarized by:

$$\frac{5}{x - 2 \bullet 2} \quad \frac{5}{2 - 2 \quad 2 \bullet 2},$$

which is very close to what we obtained for 5 5.

Configuration: 5 4_b 2

We have: $\frac{\alpha}{y \alpha y \mathbf{d}} \quad \frac{\beta \gamma}{\gamma \mathbf{d} \beta} \quad \frac{\alpha}{\mathbf{d} x \alpha x}$. This give us:

$$\frac{\alpha}{\mathbf{d} z y z} \quad \frac{y}{\mathbf{d} h y h} \quad \frac{\mathbf{d} \gamma}{k \gamma k} \quad \frac{\mathbf{d}}{t u t u} \quad \frac{\beta \mathbf{d}}{v \beta v} \quad \frac{x}{w x w \mathbf{d}} \quad \frac{\alpha}{s \alpha s \mathbf{d}} \quad \frac{x \cdot}{s \cdot \cdot}$$

with $\{y, z\} = \{s, x\} = \{\beta, \gamma\}$, $\{k, t\} = \{\alpha, \beta\}$, $\{h, k, y\} = \{v, w, x\} = \{\alpha, \beta, \gamma\}$ and $\{u, v\} = \{\alpha, \gamma\}$. A possible assortment of these variables is obtained by setting $k = u = w = \alpha$, $t = x = y = \beta$ and $h = s = v = z = \gamma$. We can summarize the results as:

$$\frac{5}{x - 2 \quad 2 \bullet 2} \quad \frac{4}{2 - 1 \bullet 1} \quad \frac{2}{1 - 5 \quad 5 \bullet y}$$

At this new step, we again have new patterns to study: 5 5_b, 2_b 1 1_b, 5_b 4 2_b, 5 1_b 5 and 1 1_b 5

Configuration: 5 5_b

We shall find a situation very similar to 5 5 and 5_b 5. We have: $\frac{\alpha}{x \alpha x \mathbf{d}} \quad \frac{\beta \gamma}{\gamma \beta \mathbf{d}}$, with $x \in \{\beta, \gamma\}$. Computations give us:

$$\frac{\cdot x}{\cdot \cdot y} \quad \frac{\alpha}{\mathbf{d} y \alpha y} \quad \frac{x}{\mathbf{d} y x y} \quad \frac{\mathbf{d} \gamma}{\alpha \gamma \alpha} \quad \frac{\beta}{\mathbf{d} u \beta u} \quad \frac{\mathbf{d} \cdot}{v \cdot v}$$

with now $\{x, y\} = \{\beta, \gamma\}$ and $\{u, v\} = \{\alpha, \gamma\}$. A possible assignment is $u = \alpha$, $x = \beta$ and $v = y = \gamma$. The result can be summarized as:

$$\frac{5}{x - 2 \quad 2 \bullet 2} \quad \frac{5}{2 - 2 \bullet 2},$$

which looks very much to the results obtained with 5 5 and 5_b 5, see Table 3.

Configuration: 2_b 1 1_b

We have: $\frac{\mathbf{d} \alpha}{\beta \alpha \beta} \quad \frac{\mathbf{d}}{\gamma y \gamma y} \quad \frac{x \mathbf{d}}{z x z}$, with $\{x, y, z\} = \{\alpha, \beta, \gamma\}$. The computations yield:

$$\frac{\cdot \beta}{\cdot \beta \mathbf{d}} \quad \frac{\alpha}{\gamma w \gamma \mathbf{d}} \quad \frac{\beta \gamma}{\gamma \beta \mathbf{d}} \quad \frac{y}{u y u \mathbf{d}} \quad \frac{\gamma}{u \gamma u \mathbf{d}} \quad \frac{y z}{z y \mathbf{d}} \quad \frac{x}{y x y \mathbf{d}} \quad \frac{z \cdot}{y \cdot \cdot}$$

with also $\{u, y\} = \{\alpha, \beta\}$ $w \in \{\alpha, \beta\}$. A possible assignment of the variables is $x = u = \alpha$, $w, y = \beta$ and $z = \gamma$. The result can be summarized by:

$$\frac{2}{5 - 5 \bullet 5} \quad \frac{1}{5 - 5 \quad 5 \bullet 5} \quad \frac{1}{5 - 5 \bullet x}$$

Configuration: $5_b \ 4 \ 2_b$

We have: $\frac{\alpha \beta}{\beta \alpha \mathbf{d}} \quad \frac{x}{y x \mathbf{d} y} \quad \frac{\mathbf{d} u}{\beta u \beta}$ where $\{u, x, y\} = \{\alpha, \gamma\}$. Computations yield:

$$\frac{\cdot \beta}{\cdot \cdot \gamma} \quad \frac{\alpha}{\mathbf{d} \gamma \alpha \gamma} \quad \frac{\mathbf{d} y}{\beta y \beta} \quad \frac{x}{\mathbf{d} z x z} \quad \frac{\mathbf{d}}{t w t w} \quad \frac{y \beta}{\beta y \mathbf{d}} \quad \frac{u}{v u v \mathbf{d}} \quad \frac{\beta \cdot}{v \cdot \cdot}$$

with $\{x, y\} = \{\alpha, \gamma\}$, $\{u, v\} = \{\alpha, \gamma\}$, $\{t, x, z\} = \{\alpha, \beta, \gamma\}$ and $\{w, y\} = \{\alpha, \gamma\}$. A possible assignment of the variables is $u = w = x = \alpha$, $t = \beta$ and $v = y = \gamma$. We can summarize the result by:

$$\frac{5}{x - 2 \bullet 2} \quad \frac{4}{2 - 2 \quad 1 \bullet 5} \quad \frac{2}{5 - 5 \bullet y}$$

Configuration: $5 \ 1_b \ 5$

We have: $\frac{\alpha}{x \alpha x \mathbf{d}} \quad \frac{\beta \mathbf{d}}{\gamma \beta \gamma} \quad \frac{r}{s r s \mathbf{d}}$, with $x \in \{\beta, \gamma\}$ and $\{r, s\} = \{\alpha, \beta\}$. Computations give us:

$$\frac{\cdot x}{\cdot \cdot y} \quad \frac{\alpha}{\mathbf{d} y \alpha y} \quad \frac{x}{\mathbf{d} y x y} \quad \frac{\mathbf{d} \gamma}{\alpha \gamma \alpha} \quad \frac{\beta}{\mathbf{d} \alpha \beta \alpha} \quad \frac{\gamma s}{\mathbf{d} s \gamma} \quad \frac{r}{\mathbf{d} \gamma r \gamma} \quad \frac{s}{\mathbf{d} t s t}$$

with $\{x, y\} = \{\beta, \gamma\}$, $\{u, x\} = \{\beta, \gamma\}$, $\{r, s\} = \{\alpha, \beta\}$ and $\{s, t, v\} = \{\alpha, \beta, \gamma\}$. A possible assignment of the variables is $r = t = \alpha$, $s = x = \beta$ and $u = v = y = \gamma$. We note that we have a new pattern which is of type 3 and it is a black node. In fact, it behaves as a white node of type 2, as shall be seen later. The results can be summarized as:

$$\frac{5}{x - 2 \quad 2 \bullet 2} \quad \frac{1}{2 - 2 \bullet 3} \quad \frac{5}{3 - 2 \quad 2 \bullet 2}$$

Configuration: $1 \ 1_b \ 5$

We have: $\frac{\mathbf{d}}{x \beta x \beta} \quad \frac{\alpha \mathbf{d}}{\gamma \alpha \gamma} \quad \frac{\alpha}{\beta \alpha \beta \mathbf{d}}$, with $x \in \{\alpha, \gamma\}$. Computations yield:

$$\frac{u \alpha}{\alpha u \mathbf{d}} \quad \frac{\beta}{\gamma \beta \gamma \mathbf{d}} \quad \frac{\alpha}{\gamma \alpha \gamma \mathbf{d}} \quad \frac{\beta \gamma}{\gamma \beta \mathbf{d}} \quad \frac{\alpha}{\beta \alpha \beta \mathbf{d}} \quad \frac{\gamma \beta}{\beta \mathbf{d} \gamma} \quad \frac{\alpha}{\mathbf{d} \gamma \alpha \gamma} \quad \frac{\beta}{\mathbf{d} u \beta u}$$

where we find that $x = \alpha$ and we need $\{u, v\} = \{\alpha, \gamma\}$. We can summarize the result as:

$$\frac{1}{5 - 5 \quad 5 \bullet 5} \quad \frac{1}{5 - 5 \bullet 4} \quad \frac{5}{4 - 2 \quad 2 \bullet 2}$$

At this step, the single new configuration is $2 \ 3_b \ 2$.

Configuration: $2 \ 3_b \ 2$

We have: $\frac{\alpha}{\mathbf{d} \gamma \alpha \gamma} \quad \frac{\beta x}{\mathbf{d} x \beta} \quad \frac{y}{\mathbf{d} z y z}$ with $\{x, y\} = \{\alpha, \gamma\}$ and $z \neq y$.

Computations yield:

$$\frac{\cdot \mathbf{d}}{s \cdot s} \quad \frac{\gamma}{r \gamma r \mathbf{d}} \quad \frac{\alpha}{\beta \gamma \beta \mathbf{d}} \quad \frac{\gamma \mathbf{d}}{\beta \gamma \beta} \quad \frac{x}{y x y \mathbf{d}} \quad \frac{\beta \mathbf{d}}{y \beta y} \quad \frac{z}{u z u \mathbf{d}} \quad \frac{y}{u y u \mathbf{d}}$$

with $\{r, s\} = \{\alpha, \beta\}$, $\{x, y\} = \{\alpha, \gamma\}$ and $\{u, y, z\} = \{\alpha, \beta, \gamma\}$. A possible assignment of the variables is $r = u = x = \alpha$, $s = z = \beta$ and $y = \gamma$. The result can be summarized by:

$$\frac{2}{1 - 5 \quad 5 \bullet 1} \quad \frac{3}{1 - 5 \bullet 1} \quad \frac{2}{1 - 5 \quad 5 \bullet x}$$

We can note that there is no new configuration and that the types generated in this case are very similar to what is produced by a sequence of consecutive nodes of type 2.

In Table 3, for each pattern, we indicate the configuration of the sons of each node of the pattern. If the nodes belonging to the pattern belong to level n of the tree, all the nodes appearing as a son of a node in the pattern are at the level $n+1$. The table numbers each pattern and, in the last columns, for each pattern p , it indicates the number of the patterns raised by p . In this way, we can see that as no new pattern appear after the 15 patterns of the table, the induction can prove that if the tiling is possible at the central cell and at the level of its immediate neighbours around it, the tiling is possible for all the next levels. This is strengthened by the fact that the colours of the sons are not completely fixed, which allows to make the choices which match with the constraints. Accordingly, this proves Theorem 5.

TABLE 3 The types of the sons of nodes with given types. The first column indicates the number of the pattern. On each line, the last column indicates the numbers of the patterns involved by the pattern described in the line.

pattern	patterns of the sons			
1	5 5	$\frac{5}{x - 2 \quad 2 \bullet 2}$	$\frac{5}{2 - 2 \quad 2 \bullet 2}$	6
2	5 5 _b	$\frac{5}{x - 2 \quad 2 \bullet 2}$	$\frac{5}{2 - 2 \bullet 2}$	6
3	5 _b 5	$\frac{5}{x - 2 \bullet 2}$	$\frac{5}{2 - 2 \quad 2 \bullet 2}$	6
4	5 4	$\frac{5}{x - 2 \quad 2 \bullet 2}$	$\frac{4}{2 - 2 \quad 1 \bullet 5}$	8
5	4 1 5	$\frac{4}{x - 2 \quad 1 \bullet 5}$	$\frac{1}{5 - 5 \quad 5 \bullet 4}$	$\frac{5}{4 - 2 \quad 2 \bullet 2}$ 9,13
6	2 2 2 _b	$\frac{2}{1 - 5 \quad 5 \bullet 1}$	$\frac{2}{1 - 5 \quad 5 \bullet 5}$	$\frac{2}{5 - 5 \bullet x}$ 12
7	2 _b 2 1	$\frac{2}{5 - 5 \bullet 1}$	$\frac{2}{1 - 5 \quad 5 \bullet 5}$	$\frac{1}{5 - 5 \quad 5 \bullet x}$
8	2 1 5 _b	$\frac{2}{1 - 5 \quad 5 \bullet 5}$	$\frac{1}{5 - 5 \quad 5 \bullet 5}$	$\frac{5}{5 - 4 \bullet 2}$ 11
9	5 4 _b 2	$\frac{5}{x - 2 \quad 2 \bullet 2}$	$\frac{4}{2 - 1 \bullet 1}$	$\frac{2}{1 - 5 \quad 5 \bullet y}$ 10,14
10	2 _b 1 1 _b	$\frac{2}{5 - 5 \bullet 5}$	$\frac{1}{5 - 5 \quad 5 \bullet 5}$	$\frac{1}{5 - 5 \bullet x}$
11	5 _b 4 2 _b	$\frac{5}{x - 2 \bullet 2}$	$\frac{4}{2 - 2 \quad 1 \bullet 5}$	$\frac{2}{5 - 5 \bullet y}$ 7
12	5 1 _b 5	$\frac{5}{x - 2 \quad 2 \bullet 2}$	$\frac{1}{2 - 2 \bullet 3}$	$\frac{5}{3 - 2 \quad 2 \bullet 2}$ 15
13	5 4 _b 2	$\frac{5}{x - 2 \quad 2 \bullet 2}$	$\frac{4}{2 - 1 \bullet 1}$	$\frac{2}{1 - 5 \quad 5 \bullet y}$ 10,14
14	1 1 _b 5	$\frac{1}{5 - 5 \quad 5 \bullet 5}$	$\frac{1}{5 - 5 \bullet 4}$	$\frac{5}{4 - 2 \quad 2 \bullet 2}$ 13
15	2 3 _b 2	$\frac{2}{1 - 5 \quad 5 \bullet 1}$	$\frac{3}{1 - 5 \bullet 1}$	$\frac{2}{1 - 5 \quad 5 \bullet x}$ 12



References

- [1] C. Carathéodory. Theory of functions of a complex variable, vol.II, 177–184, Chelsea, New-York, 1954.
- [2] H. S. M. Coxeter, W. O. J. Moser, *Generators and Relations for Discrete Groups*, II Ed., Springer, Berlin, (1965).
- [3] D. B. A. Epstein, J. W. Cannon, D. F. Holt, S. V. F. Levi, M. S. Paterse, W. P. Thurston, *Word Processing in Groups*, Jones and Barlett Publ., Boston, (1992).
- [4] K. Imai, H. Ogawa, A simulating tool for hyperbolic cellular automata and its application to construct hyperbolic cellular automata which can simulate logical circuits, Proceedings of CA 2000, International Workshop on Cellular Automata, Sixth IFIP WG1.5 Meeting, August 21-22, 2000, Osaka, Japan, 11–11.
- [5] C. Mann, On Heesch’s problem and other tiling problems, PhD Thesis, University of Arkansas, (2001).
- [6] Margenstern M., Cellular automata in the hyperbolic plane, Technical report, Publications du GIFM, I.U.T. of Metz, N°99-103, ISBN 2-9511539-3-7, 34p. 1999.
- [7] Margenstern M., Cellular automata in the hyperbolic plane (II), Technical report, Publications du GIFM, I.U.T. of Metz, N°2000-101, ISBN 2-9511539-7-X, 40p. 2000.
- [8] Margenstern M., New Tools for Cellular Automata of the Hyperbolic Plane, *Journal of Universal Computer Science* **6**No12, 1226–1252, (2000)
- [9] Margenstern M., Tiling the hyperbolic plane with a single pentagonal tile, École de Printemps, PAVAGES’2000, Branville, France, may 2000.
- [10] Margenstern M., Tiling the hyperbolic plane with a single *à la* Wang tile, technical report, Publications du LITA, Université de Metz, N° 2001-101, 61pp, (2001).
- [11] Margenstern M., Morita K., NP problems are tractable in the space of cellular automata in the hyperbolic plane. Technical report, Publications of the I.U.T. of Metz, 38p. 1998.
- [12] Margenstern M., Morita K., A Polynomial Solution for 3-SAT in the Space of Cellular Automata in the Hyperbolic Plane, *Journal of Universal Computations and Systems*,
- [13] Margenstern M., Morita K., NP problems are tractable in the space of cellular automata in the hyperbolic plane, *Theoretical Computer Science*, **259**, 99–128, (2001)

- [14] Margenstern M., Skordev G., Locating cells in regular grids of the hyperbolic plane for cellular automata, Technical report, N° 455, July 2000, Institut für Dynamische Systeme, Fachbereich Mathematik/Informatik/Technomathematik, Universität Bremen, 2000, 38p.
- [15] Margenstern M., Subramanian K.G. Hyperbolic tiling and formal language theory, *Electronic Proceedings in Theoretical Computer Science* 128, pp. 128-136, (2013).
- [16] M. Margenstern, Cellular Automata in Hyperbolic Spaces, volume 1, Theory, *Old City Publishing*, Philadelphia, (2007), 422p.
- [17] M. Margenstern, Cellular Automata in Hyperbolic Spaces, volume 2, Implementation and Computations, *Old City Publishing*, Philadelphia, (2008), 360p.
- [18] M. Margenstern, Small Universal Cellular Automata in Hyperbolic Spaces, A Collection of Jewels, *Collection: Emergence, Complexity and Computation*, Springer, (2013), 320p.
- [19] Novikov P.S., On the algorithmic unsolvability of the word problem in group theory. Trudy Matematicheskogo Instituta imeni Steklova, **44**, (1955) (English translation in American Mathematical Society Translations (2) **9**, (1958)).
- [20] Poincaré H., Théorie des groupes fuchsien. *Acta Mathematica*, **1**, 1–62, (1882).
- [21] D. E. Muller and P. E. Schupp, Groups, the theory of ends, and context-free languages, *J. Comput. System Sci.* 26 (1983) 295-310.
- [22] D. E. Muller and P. E. Schupp, The theory of ends, pushdown automata, and second-order logic, *Theoretical Computer Science* 37 (1985) 51-75.
- [23] M. Dehn Über unendliche diskontinuierliche Gruppen, *Mathematische Annalen* 71 (1) 116-144.
- [24] M. Dehn, Transformation der Kurven auf zweiseitigen Flächen, *Mathematische Annalen* 72 (3) 413-421.